Chapter 7

Thermal Oxidation Mechanism of Silicon Carbide

Yasuto Hijikata, Shuhei Yagi, Hiroyuki Yaguchi and Sadafumi Yoshida

Additional information is available at the end of the chapter

http://dx.doi.org/10.5772/50748

1. Introduction

Recently, semiconductor devices that work normally for a long time under harsh environments are demanded such as in nuclear power application or in space development field. Especially, after the disaster of Fukushima Dai-ichi nuclear power plant caused by the East-Japan great earthquake on March 11, 2011, the importance of such a *hard* electronic devices has been growing. However, it is difficult to achieve the performance using conventional semiconductors such as Si semiconductor because of its physical property limit.

Prevention of the global warming is one of the most important and urgent subjects in the world. Technologies to reduce energy consumption should be the key for overcoming this problem, and one of which is the improvement in the efficiency of power devices.

Silicon carbide (SiC) semiconductor is one of the wideband gap semiconductors and the use of it is considered as the solution to achieve these performances because it has superior physical properties such as 3 times wider bandgap, 10 times larger electrical break-down field, and 3 times higher thermal conductivity, compared with Si semiconductor [1]. Taking advantages of these properties, on-resistance for unipolar devices such as metal-oxide-semiconductor field-effect-transistors (MOSFETs) can, for example, be reduced by a factor of a few hundreds when replacing Si with SiC semiconductor. In addition, SiO_2 film, utilized as an insulator in MOSFETs, can be grown on the SiC substrate surface by thermal oxidation, which is well compatible with the Si MOS device technologies [2]. Moreover, the power and frequency ranges of SiC MOSFETs are around 1 kV break-down voltage and around 20 kHz switching frequency, respectively, which covers the wide power device application field.

For these reasons, the developments of SiC power MOSFETs have been very popular for a few decades. However, the on-resistances for MOSFETs fabricated practically are beyond the lower limit for Si, however, higher than the SiC limit by a few orders [3]. As a result, conven-

tional Si insulated gate bipolar transistors (IGBTs) still have most of the share in the application fields of power transistors. In the case of 1 kV break-down voltage device, the channel resistance is dominant to the total on-resistance. Therefore, controlling the channel layer, *i.e.* the SiC-SiO_2 interface structure, should be the key technology to realize a SiC -MOSFET with desired performances. Besides, although the long-term reliability of oxide is very important for the practical uses of MOSFETs, that of SiC MOS device are still lower than that of Si by a factor of 1 order. As the creation of interface layers and the characteristics of oxide layers are closely related to the growth mechanism of the oxide, it is safely said that the observation of SiO_2 growing process is very significant work for overcoming these problems.

In previous work, we have, for the first time, performed real-time observation of SiC thermal oxidation using an *in-situ* ellipsometer [4, 5]. The results show that the oxidation-time dependence of oxide thickness can essentially be represented by the Deal-Grove (D-G) model [6], which has been originally proposed for the explanation of Si oxidation. Song *et al.* [7] have modified the D-G model for applying it to SiC oxidation, taking the process of carbon oxidation into account. They have concluded that a linear-parabolic formula can also be applicable to SiC oxidation, although the parabolic term includes the contribution from the diffusion of CO or CO_2 molecules from the SiC-oxide interface to the surface as well as that of oxygen from the surface to the interface. However, our further studies have found that the oxide growth rates in the thin oxide region are higher than those predicted from the D-G model [4, 8, 9, 10, 11]. By the way, it is well known that also the oxidation behavior of Si cannot be explained using the D-G model, *i.e.*, particularly at the initial oxidation stage. Accordingly, several models that describe Si oxidation have been proposed [12, 13, 14, 15, 16].

At the beginning of this chapter, we review the thermal oxidation models for SiC as well as those for Si that have been previously proposed, to elucidate the oxidation mechanism of SiC and then we verify each of these SiC oxidation models by making comparison with the oxide growth rate data with various oxidation conditions and discuss the structure and nature of the SiC-oxide interface layer based on the oxidation model that we have proposed.

2. Thermal oxidation models for Si and SiC

2.1. Deal-Grove model and its related models

The kinetic model of Si oxidation that is most often taken as a reference is the one so-called Deal-Grove model proposed by Deal and Grove [6, 12]. According to this model, the beginning of oxidation is limited to the interfacial oxidation reaction and, after oxidation proceeds, the rate-imiting process is transferred from the interfacial reaction to the diffusion of oxidants in SiO_2. This process is expressed by the following equation given by Deal and Grove as [6, 12]

$$\frac{dX}{dt} = \frac{B}{A + 2X} \tag{1}$$

http://dx.doi.org/10.5772/50748

where B/A and B are denoted as the linear and parabolic rate constants of oxidation, respectively. It is noted that B/A and B are the rate coefficients for the interfacial reaction and the diffusion of oxidants, respectively, *i.e.*,

$$\frac{B}{A}=\frac{kC_O^0}{N_0},\ B=\frac{2D_OC_O^0}{N_0} \tag{2}$$

where k is the interfacial oxidation rate constant, C^0 the solubility limit in SiO_2, N_0 the molecular density of SiO_2, D the diffusivity in SiO_2, and the subscript means the value for the corresponding atom. By the way, according to the definition in the D-G model, in which the oxide growth proceeds under steady-state and a SiO_2 film is grown only at the SiO_2-Si interface, the equation (1) can also be written as [6, 12]:

$$\frac{dX}{dt}\equiv\frac{kC_O^I}{N_0}\left(=\frac{k}{N_0}\frac{C_O^0}{(k/D_O)X+1}\right) \tag{3}$$

where C^I is the atomic concentration at the interface. Comparing eq. (3) with eqs. (1, 2), $C_O^I$is almost constant by C_O^0 while $X\le D_O/k$ and, in turn, it reduces inverse proportional to X when $X>D_O/k$ (see the right-end parentheses in eq. (3)). Therefore, we can see that the length $D_O/k(=A/2)$ corresponds to the thickness at which the interfacial reaction rate-limiting step transits to the diffusion of oxidants one. On the contrary, Watanabe *et al.* reconfirmed the validity of eq. (1), but modified the framework of A parameter, based on the consideration that the growth rate at the full range of oxide thickness is limited by the oxygen diffusion, *i.e.*, there is no interfacial reaction-limited step in the Si oxidation process [16].

2.2. Massoud empirical relation

It is well known that, in the case of dry oxidation, the oxidation rate of Si in the thin oxide thickness range cannot be reproduced by the D-G equation [6, 12] and, hence, several models to describe the growth rate enhancement in the thin oxide regime have been proposed. Among them, Massoud *et al.* [13] have proposed an empirical relation for the oxide thickness dependence of oxidation rate, that is, the addition of an exponential term to the D-G equation,

$$\frac{dX}{dt}=\frac{B}{A+2X}+C\exp\left(-\frac{X}{L}\right) \tag{4}$$

where C and L are the pre-exponential constant and the characteristic length, respectively. Also in the case of SiC oxidation, we have found that it is possible to fit the calculated values to the observed ones using eq. (4) much better than using eq. (1) regardless of oxidation temperature, as shown in Fig. 1. However, this empirical equation can only reproduce the observed growth rates numerically, but does not provide a physical meaning.

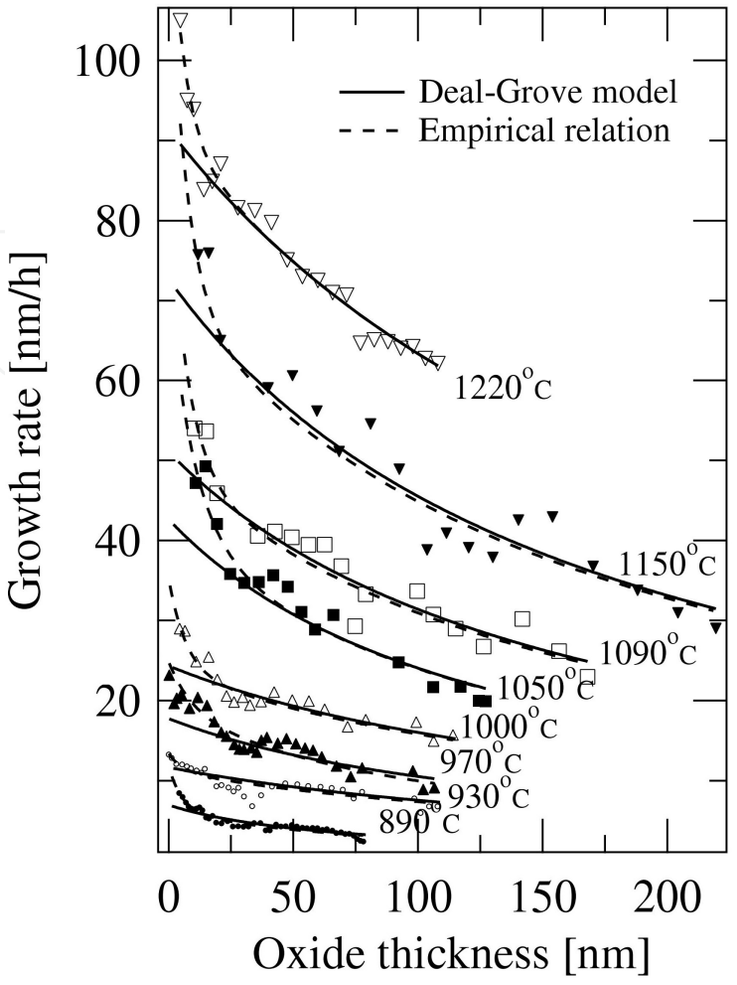

Figure 1. Oxide thickness dependences of oxidation rate at various oxidation temperatures on (000$\bar{1}$) C-face. The solid and dashed lines denote the values derived from the Deal-Grove model (eq. (1) [6]) and those from the empirical relation (eq. (4) [13]), respectively.

2.3. Interfacial Si emission model for Si

Some Si oxidation models that describe the growth rate enhancement in the initial stage of oxidation have been proposed [14, 15, 17]. The common view of these models is that the stress near/at the oxide-Si interface is closely related to the growth enhancement. Among these models, the 'interfacial Si emission model' is known as showing the greatest ability to fit the experimental oxide growth rate curves. According to this model, Si atoms are emitted as interstitials into the oxide layer accompanied by oxidation of Si, which is caused by the strain due to the expansion of Si lattices during oxidation. The oxidation rate at the interface (k in eq. (2)) is initially large and is suppressed by the accumulation of emitted Si atoms near the interface with increasing oxide thickness, *i.e.*, the k is not constant but a function of oxide thickness and the oxidation rate is not enhanced in the thin oxide regime but is quickly suppressed with increasing thickness. To describe this change in the interfacial reaction rate, Kageshima *et al.* introduce the following equation as the interfacial reaction rate, k [14, 17]:

http://dx.doi.org/10.5772/50748

$$k = k_0\left(1 - \frac{C_{Si}^{I}}{C_{Si}^{0}}\right) \tag{5}$$

where k_0 is the initial interfacial oxidation rate.

In the D-G model and the Massoud empirical relation, it has been considered that oxide growth occurs only or mainly at the Si-oxide interface. However, according to the interfacial Si emission model [14], Si atoms are emitted into the oxide layer, some of which encounter the oxidant inside the SiO_2 layer to form SiO_2. In addition to this, when the oxide is very thin, some of the emitted Si atoms can go through the oxide layer and reach the oxide surface, and are instantly oxidized, resulting in the formation of an SiO_2 layer on the oxide surface. Therefore, there are two oxide growth processes other than the interfacial oxide growth, *i.e.*, oxide formation due to oxidation of Si interstitials inside the oxide and on the oxide surface. The total growth rate is given by the sum of these three oxidation processes, as [14],

$$N_0\frac{dX}{dt} = kC_O^{I}(1 - \nu_{Si}) + \int_0^X \kappa(C_O)^2 C_{Si}\,dx + \eta(C_O^{S})^2 C_{Si}^{S} \tag{6}$$

where the ν is the emission ratio, the κ is the oxidation rate of Si interstitials inside SiO_2, $\eta$is the oxidation rate of Si interstitials on the oxide surface, and the superscript 'S' means the position at the oxide surface (x=X). The first, second, and third term in the right-hand side of eq. (6) correspond to the interfacial oxide growth, the oxide growth inside SiO_2, and that on the oxide surface, respectively. The concentrations of Si interstitials and O_2 moleculers in SiO_2 (C_{Si} and C_O, respectively) are derived using a numerical calculation based on the diffusion theory [17]. The diffusion equations will be shown in Sec. 2.4. If the steady-state approximation is assumed for the calculation, the obtained growth rate equation is equivalent to the Massoud empirical relation [14].

2.4. Si and C emission model for SiC

Since the density of Si atoms in 4H-SiC (4.80×10^{22}cm^{-3} [18]) is almost the same as that in Si (5×10^{22}cm^{-3}) and the residual carbon is unlikely to exist at the oxide-SiC interface in the early stage of SiC oxidation, the stress near/at the interface is considered to be almost identical to the case of Si oxidation. Therefore, it is probable that atomic emission due to the interfacial stress also accounts for the growth enhancement in SiC oxidation. In addition, in the case of SiC oxidation, we should take C emission as well as Si emission into account because SiC consists of Si and C atoms.

Recently, we have proposed a SiC oxidation model, termed "Si and C emission model", taking the Si and C emissions into the oxide into account, which lead to a reduction of interfacial reaction rate [19]. Figure 2. schematizes the Si and C emission model. Considering Si and C atoms emitted from the interface during the oxidation as well as the oxidation process of C, the reaction equation for SiC oxidation can be written as,

$$\mathrm{SiC}+\left(2-\nu_{\mathrm{Si}}-\nu_{\mathrm{C}}-\frac{\alpha}{2}\right)\mathrm{O}_2\rightarrow(1-\nu_{\mathrm{Si}})\mathrm{SiO}_2+\nu_{\mathrm{Si}}\mathrm{Si}+\nu_{\mathrm{C}}\mathrm{C}+\alpha\mathrm{CO}+(1-\nu_{\mathrm{C}}-\alpha)\mathrm{CO}_2 \tag{7}$$

where α denotes the production ratio of CO.

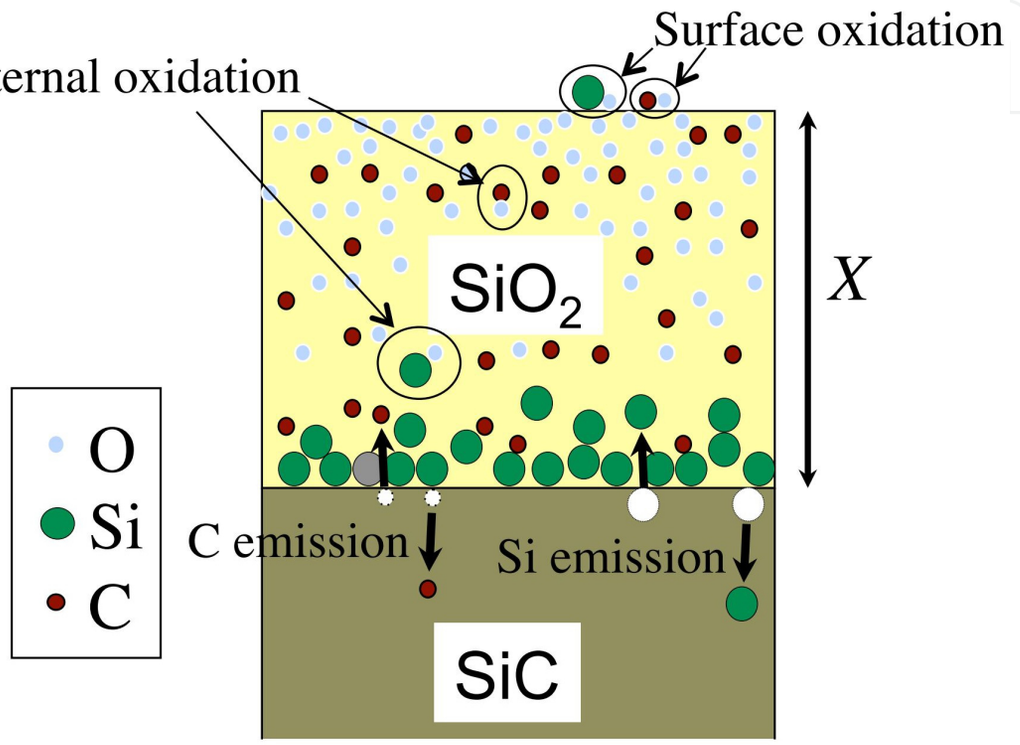

Figure 2. Schematic illustration of the Si and C emission model [19]. It is to be noted that Si and C atoms are practically emitted into not only to the SiO_2-side, but also the SiC-side, as shown in the figure.

In the case of Si oxidation, the interfacial reaction rate (eq. (5)) is introduced by assuming that the value of $C_{\mathrm{Si}}^{\mathrm{I}}$ does not exceed the C_{Si}^{0} though the reaction rate decreases with increase of$C_{\mathrm{Si}}^{\mathrm{I}}$. Based on this idea, the interfacial reaction rate for SiC is thought to be given by multiplying decreasing functions for Si and C [19]:

$$k=k_0\left(1-\frac{C_{\mathrm{Si}}^{\mathrm{I}}}{C_{\mathrm{Si}}^{0}}\right)\left(1-\frac{C_{\mathrm{C}}^{\mathrm{I}}}{C_{\mathrm{C}}^{0}}\right) \tag{8}$$

This equation implies that the growth rate in the initial stage of oxidation should reduce by two steps because the accumulation rates for Si and C interstitials should be different from each other, and hence, the oxidation time when the concentration of interstitial saturates should be different between Si and C interstitial. This prediction will be evidenced in the next section.

http://dx.doi.org/10.5772/50748

Diffusion equations for Si and C interstitials, and oxidants can be written by modifying the those given by the interfacial Si emission model [17], that is,

$$\begin{aligned}
&\frac{\partial C_{\mathrm{Si}}}{\partial t}=\frac{\partial}{\partial x}\left(D_{\mathrm{Si}}\frac{\partial C_{\mathrm{Si}}}{\partial x}\right)-R_1-R_2,\\
&R_1=\eta C_{\mathrm{O}}^{\mathrm{S}}C_{\mathrm{Si}}^{\mathrm{S}},\ R_2=\kappa_1 C_{\mathrm{Si}}C_{\mathrm{O}}+\kappa_2 C_{\mathrm{Si}}(C_{\mathrm{O}})^2,\\
&\frac{\partial C_{\mathrm{C}}}{\partial t}=\frac{\partial}{\partial x}\left(D_{\mathrm{C}}\frac{\partial C_{\mathrm{C}}}{\partial x}\right)-R_1^{'}-R_2^{'},\\
&R_1^{'}=\eta^{'}C_{\mathrm{O}}^{\mathrm{S}}C_{\mathrm{C}}^{\mathrm{S}},\ R_2^{'}=\kappa_1^{'}C_{\mathrm{C}}C_{\mathrm{O}}+\kappa_2^{'}C_{\mathrm{C}}(C_{\mathrm{O}})^2,\\
&\frac{\partial C_{\mathrm{O}}}{\partial t}=\frac{\partial}{\partial x}\left(D_{\mathrm{O}}\frac{\partial C_{\mathrm{O}}}{\partial x}\right)-R_1-R_2-R_1^{'}-R_2^{'}-R_3,\\
&R_3=h\left(C_{\mathrm{O}}^{\mathrm{S}}-C_{\mathrm{O}}^{0}\right)
\end{aligned}\tag{9}$$

where the prime means the variation for C atoms. It is noted that the R_2 and $R_2^{'}$ mean absorption of interstitials inside the oxide and they are assumed to be consist of two terms, as suggested by Uematsu *et al.* [20]. From eq. (7), the boundary conditions at the interface are given as,

$$\begin{aligned}
&D_{\mathrm{Si}}\frac{\partial C_{\mathrm{Si}}}{\partial x}\Big|_{x=0}=-v_{\mathrm{Si}}kC_{\mathrm{O}}^{\mathrm{I}},\ D_{\mathrm{C}}\frac{\partial C_{\mathrm{C}}}{\partial x}\Big|_{x=0}=-v_{\mathrm{C}}kC_{\mathrm{O}}^{\mathrm{I}},\\
&D_{\mathrm{O}}\frac{\partial C_{\mathrm{O}}}{\partial x}\Big|_{x=0}=\left(2-v_{\mathrm{Si}}-v_{\mathrm{C}}-\frac{\alpha}{2}\right)kC_{\mathrm{O}}^{\mathrm{I}}
\end{aligned}\tag{10}$$

It has been believed that the oxidation rate in the thick oxide regime is solely limited by the in-diffusion of oxidant and the diffusivity of CO in SiO_2 is much larger than that of O_2. Thus, we assumed that the diffusion process of CO is insensitive to the oxide growth rate. The oxide growth rate is described as eq. (6), but the second term in the right-hand side (*i.e.* the absorption-term of Si interstitials inside the oxide) is modified to be the combination of κ_1 and κ_2 shown in eq. (9) (see eq. (6) in Ref. [19]). We approximated this integral term by the area of a triangle $C_{\mathrm{Si}}^{\mathrm{I}}$ in height and $\partial C_{\mathrm{Si}}/\partial x\,|_{x=0}\,/2$ in gradient of hypotenuse, on the basis of the idea that interstitials are usually distributed according to what resembles a complementary error function or exponential function, and their areal density is given approximately by the area of the triangle [21].

Equations (8-10) were solved numerically using the partial differential equation solver ZOMBIE [22]. The oxide thickness, X, at each time step was obtained from eq. (6). The parameters related to the properties of SiO_2 (D_{Si},D_{O} , η, κ_1, $\kappa_2$andC_{Si}^{0}) were set to the same values as those obtained for Si oxidation [17]. The parameters concerning C interstitials (α, v_{C}, D_{C}, $\eta^{'}$, $\kappa_1^{'}$, $\kappa_2^{'}$andC_{C}^{0}) as well as the values of k_0 and v_{Si} were determined by fitting the calculated oxide growth rates to the measured ones.

3. Results and Discussion

3.1. Differences in the oxidation process between C- and Si-face

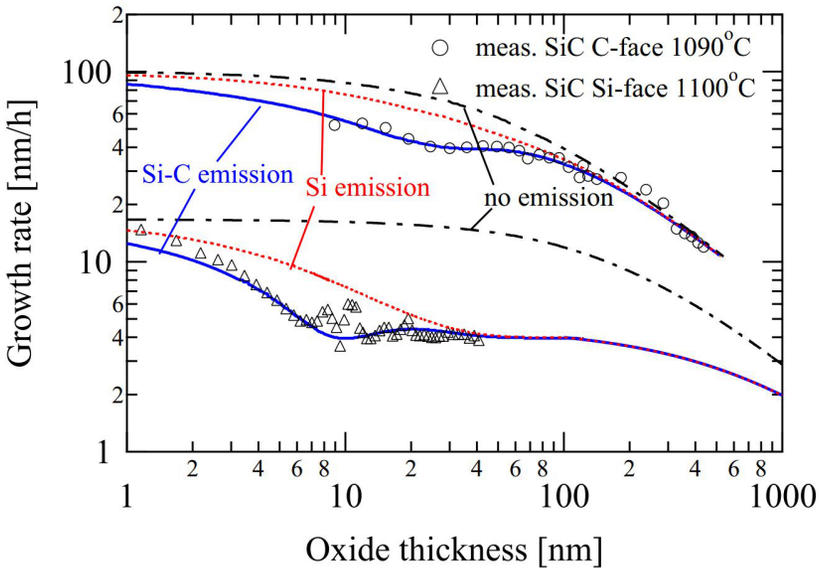

Figure 3. Oxide thickness dependence of growth rates on C- and Si-faces.

Figure 3 shows the oxide growth rates observed for 4H-SiC C face at 1090°C (circles) and Si face at 1100°C (triangles). The oxide growths were executed under dry oxygen ambient at a pressure of 1 atm. The experimental details can be found in the references [8, 9, 10]. Also shown in the figure are the growth rates given by the Si and C emission model (blue solid lines), the Si emission model, and the model that does not take account of both Si and C emission, *i.e.*, the D-G model (red broken line and black double broken line, respectively). We note that the same parameters were used for these three SiC oxidation models.

Figure 3 shows that the Si and C emission model reproduces the experimental values for both the C and Si faces better than the other two models. In particular, the dip in the thickness dependence of the growth rate seen around 20 nm for the C-face and 10 nm for the Si-face, which cannot be reproduced by the Si emission model or the D-G model no matter how well the calculation are tuned, can be well reproduced by the Si and C emission model. These results suggest that the C interstitials play an important role in the reduction of the oxidation rate, similarly to the role of the Si interstitials. Moreover, from the fact that the drop in growth rate in the initial stage of oxidation is larger for the Si and C emission model than in the case of taking only Si emission into account, we found that the accumulation of C interstitials is faster than that of Si interstitials and that the accumulation of C interstitials is more effective in the thin oxide regime.

As mentioned in Sec. 2.1, the growth rate in the thick oxide regime is determined by the parabolic rate constant B as is obvious if we consider the condition that $A \ll 2X$ for eqs. (1, 4). Song *et al.* proposed a modified Deal-Grove model that takes the out-diffusion of CO into ac-

count by modifying the parabolic rate constant B by a factor of 1.5 (called 'normalizing factor' [23]), and through this model, they explained the oxidation process of SiC in the parabolic oxidation rate regime [7]. For the Si and C emission model, the normalizing factor corresponds to the coefficient of the oxidant shown in eq. (7), *i.e.* $(2-\nu_{Si}-\nu_C-\alpha/2)$. Since Song's model assumed that there is no interfacial atomic emission (*i.e.* $\nu_{Si}=\nu_C=0$) and carbonaceous products consist of only CO (*i.e.* $\alpha=1$), for this case, the coefficient of the oxidant in eq. (7) equals 1.5, which is the same as the normalizing factor. Actually, our experiments revealed this coefficient to be 1.53 [19], which is almost equal to the measured value from Song *et al.* Therefore, our results support the assumption in the Song's model that $\alpha=1$ and we believe that the obtained B values to be different from that of Si oxidation [5, 7, 23, 24] despite the fact that the native oxide is SiO_2 regardless of Si and SiC were due to the contribution from CO production in SiC oxidation. While in the case of the Si-face, since the influence of oxygen diffusion was significant at thicknesses above several μm as seen in Fig. 3, we could not determine the value ofα. The value of α is thought to depend on the areal density of carbon in the substrate. Thus, we regard the α value of the Si-face as equal to that of C-face.

The parameters to be different between C- and Si-face in the deduced values wereν_{Si}, ν_C, and k_0. In next section, we will discuss the temperature dependence of these three parameters.

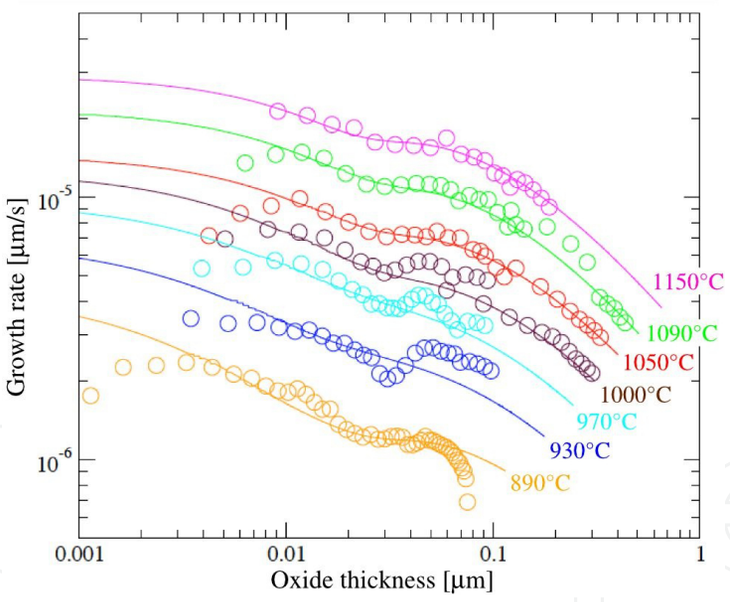

Figure 4. Oxide thickness dependence of oxide growth rates at various oxidation temperatures for $(000\bar{1})$C-face. The circles and the solid curves denote measured growth rates and calculated ones, respectively.

3.2. Oxidation rate at various oxidation temperatures

Figure 4 shows the oxide growth rates as a function of oxide thickness, observed for the dry oxidation of C-face at various oxidation temperatures (circles) and those given by the Si and C emission model (the solid curves) [25]. The figure indicates that the Si and C emission model reproduces the oxide growth rate curves for all of the temperatures measured. As

mentioned above, some articles have suggested that [7, 23, 26] the SiC oxidation can be described by using the D-G model. However, there are several issues in the application of D-G model to SiC oxidation, in which unreasonable parameter values are needed to fit to the measured oxide growth rates. For example, the activation energy of parabolic oxidation-rate constant B for SiC Si-face and $(11\bar{2}0)\alpha$ -face significantly different from that for Si is required to fit the growth rate curve despite the fact that both of oxides on SiC and Si are SiO_2. In accordance with Si and C emission model, on the contrary, the oxide growth rates of SiC for all of the temperatures measured can be derived using just the same diffusivities as those for Si regardless of oxidation temperatures. This shows that the Si and C emission model is more valid than the D-G model to explain SiC oxidation process.

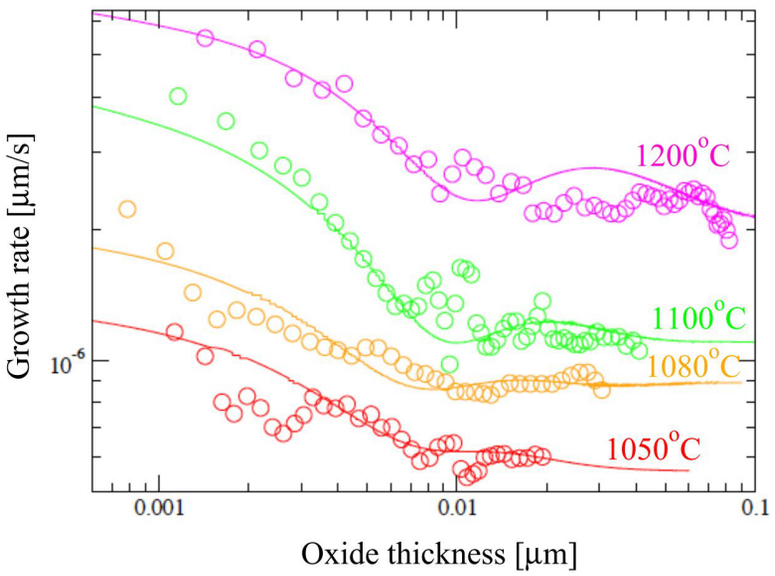

Figure 5. Oxide thickness dependence of oxide growth rates at various oxidation temperatures for (0001)Si-face. The circles and the solid curves denote measured growth rates and calculated ones, respectively.

Figure 5 shows the oxide growth rates for Si-face as a function of the oxide thickness at various oxidation temperatures. The calculated curves also well agree with the measured data. The figure indicates that the values obtained are almost constant in the larger thickness range in this study at any oxidation temperature. The reason for this constant thickness dependence is that, in the case of Si-face, interfacial reaction rate-limiting step continues up to several μm in oxide thickness, as revealed in Sec. 3.1.

Figure 6 shows the temperature dependence of Si and C emission ratios (ν_{Si}andν_C, respectively) and initial interfacial reaction rate (k_0) for C- and Si-face deduced from the curve fits. The figure indicates that the activation energies of $\nu_{Si}$and ν_C are comparable between these polar faces, but the values of them for Si-face are larger than those for C-face, in particular, the ν_{Si} for Si-face is remarkably large. It is noted that the ν_{Si} values for C-face were just the same as those for Si(100)face. On the other hand, the activation energy of k_0 is a little larger for Si-face, while the k_0 values for these faces approach each other as elevating temperature.

http://dx.doi.org/10.5772/50748

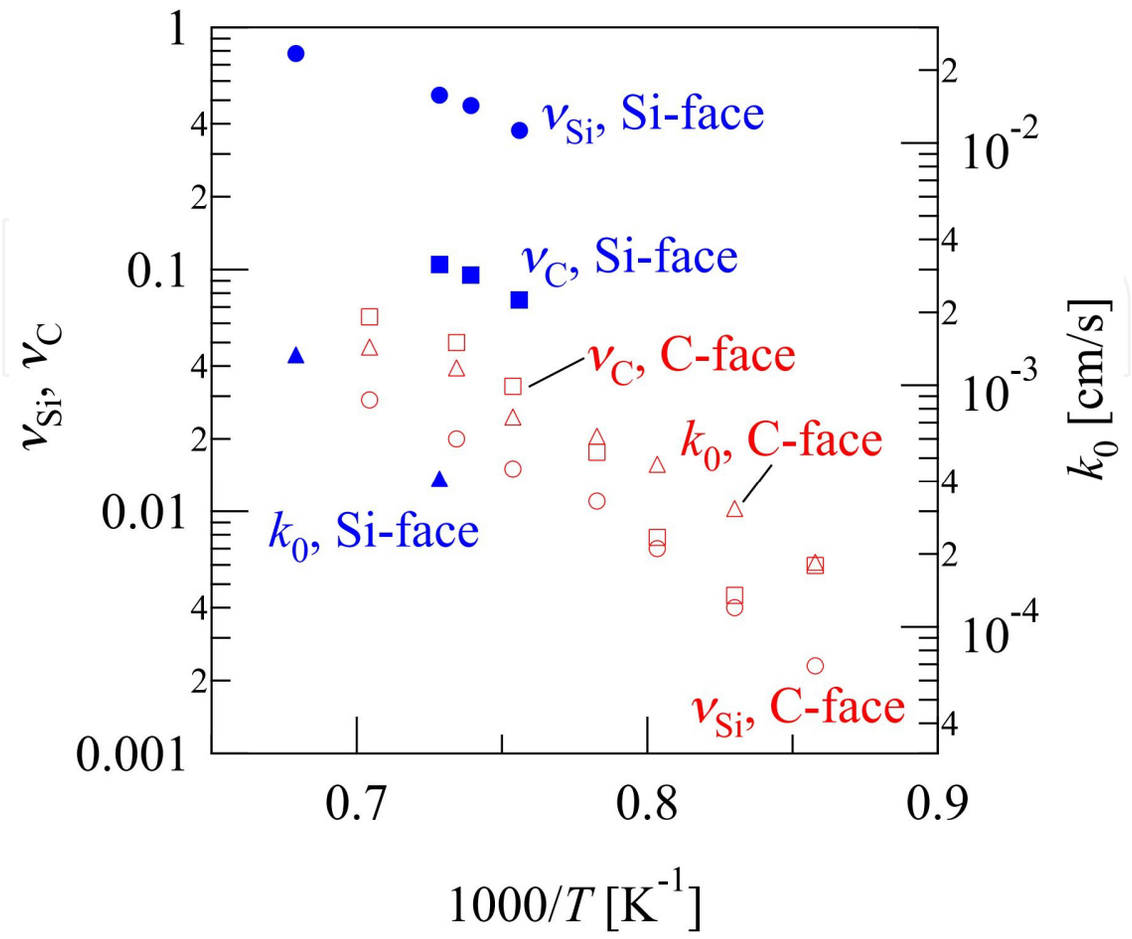

Figure 6. Arrehnius plots ofν_{Si}, ν_C, and k_0 (circles, squares, and triangles, respectively) for Si- and C-face.

In the simulation for Si oxidation, Uematsu *et al.* have found that the ν_{Si} depends on surface orientation of the substrate [17]. Therefore, it is possible that the differences in ν_{Si} and ν_C also appear between SiC C- and Si-face. Obviously, a high Si emission ratio leads to a low oxide growth rate, as shown in eqs. (5, 8). Therefore, it is considered that the high Si emission ratio is one of the causes for the low oxidation rate for Si-face [28]. Uematsu *et al.* also found that the k_0 also depends on surface orientation, which is probably due to the difference in surface density of the Si-Si bonds available for the reaction with oxidants [17]. In the case of SiC, the areal density of such reaction-available bonds on Si-face is lower than that on C-face by a factor of three, which is roughly coincident with the difference in observed data (Fig. 6). According to the report from Ref. [27], in the cases of extremely high oxidation temperature (~1500°C), the oxide growth rate is comparable between C- and Si-face, which is different from the fact that the oxide growth rates for the C-face are about eight times larger than those for the Si-face in the several 10 nm thickness region at around 1100°C and atmospheric oxygen pressure. We consider that such a high temperature oxidation proceeds with another mechanism such as 'active oxidation' (*i.e.* oxidizing with evaporation), so that the substrate orientation does not affect the oxidation process any more.

for SiC	
$\eta'[\mathrm{cm}^3\cdot\mathrm{s}^{-1}]$	$*\,5\times10^{-8}$
$D_C[\mathrm{cm}^2\cdot\mathrm{s}^{-1}]$	$2.0\times10^{-9}\exp(-0.57\mathrm{eV}/k_BT)$
$\kappa_1'[\mathrm{cm}^3\cdot\mathrm{s}^{-1}]$	$1.04\times10^{-15}\exp(-1.55\mathrm{eV}/k_BT)$
$\kappa_2'[\mathrm{cm}^6\cdot\mathrm{s}^{-1}]$	$1.04\times10^{-32}\exp(-1.55\mathrm{eV}/k_BT)$
$C_C^0[\mathrm{cm}^{-3}]$	$3.6\times10^{23}\exp(-1.07\mathrm{eV}/k_BT)$
common values	
$\eta[\mathrm{cm}^3\cdot\mathrm{s}^{-1}]$	5×10^{-8}
$D_{Si}[\mathrm{cm}^2\cdot\mathrm{s}^{-1}]$	$8.1\times10^{-2}\exp(-3.43\mathrm{eV}/k_BT)$
$\kappa_1[\mathrm{cm}^3\cdot\mathrm{s}^{-1}]$	$1.46\times10^{-14}\exp(-1.55\mathrm{eV}/k_BT)$
$\kappa_2[\mathrm{cm}^6\cdot\mathrm{s}^{-1}]$	$1.46\times10^{-31}\exp(-1.55\mathrm{eV}/k_BT)$
$D_O[\mathrm{cm}^2\cdot\mathrm{s}^{-1}]$	$1.3\times10^{-2}\exp(-1.64\mathrm{eV}/k_BT)$
$C_{Si}^0[\mathrm{cm}^{-3}]$	$3.6\times10^{24}\exp(-1.07\mathrm{eV}/k_BT)$
$C_O^0[\mathrm{cm}^{-3}]$	5.5×10^{16}
*Assumed value	

Table 1. Arrehnius equations used for the calculations of SiC oxide growth rate. The common values for SiC and Si are extracted from the reference [17].

In the oxide growth calculations, we gave the same parameters to C- and Si-face in the case that the parameters are related to SiO_2 (*i.e.* η', D_C, κ_1', κ_2', andC_C^0). Through the curve fits for various oxidation temperatures, we obtained their Arrehnius equations. Table 1 addresses the Arrehnius equations for these common parameters such as D_C as well as those related to the properties of SiO_2 from Ref. [17]. It is noticed that the self-diffusivities of Si and O (D_{Si}^{SD} andD_O^{SD}, respectively, in Ref. [17]) have been transformed to ordinary diffusivities. Looking at the table, the activation energy of D_C (0.57 eV) seems to be small. Indeed, *ab-initio* studies have reported the energy between 2-3 eV [29]. We suppose for this discrepancy that our obtained value originates from not a segregation but a migration, that is, it is the diffusivity for C atoms that diffuse as interstitials. Note that the calculated growth rates are quite insensi-

http://dx.doi.org/10.5772/50748

tive to the variation of η and η' when these values are large enough to sink all the intersti-

tials that reach the oxide surface.

3.3. Oxidation rate at various oxygen partial pressures

To determine the oxygen pressure dependence of the SiC oxidation process, *ex-situ* measure-

ments from 10^{-3} to 4 atm have been carried out [23, 27]. However, both of these studies did

not examine the initial oxidation process in detail, partly because *in-situ* real-time observa-

tions were not possible. We performed *in-situ* real-time measurements at reduced partial

pressures between 0.1 and 1.0 atm, and found the presence of the initial growth rate en-

hancement to be similar to the case at atmospheric pressure [10]. Recently, we observed the

SiC oxidation process under low oxygen partial pressures down to 0.02 atm to examine the

initial stage of oxidation in more detail [11, 30].

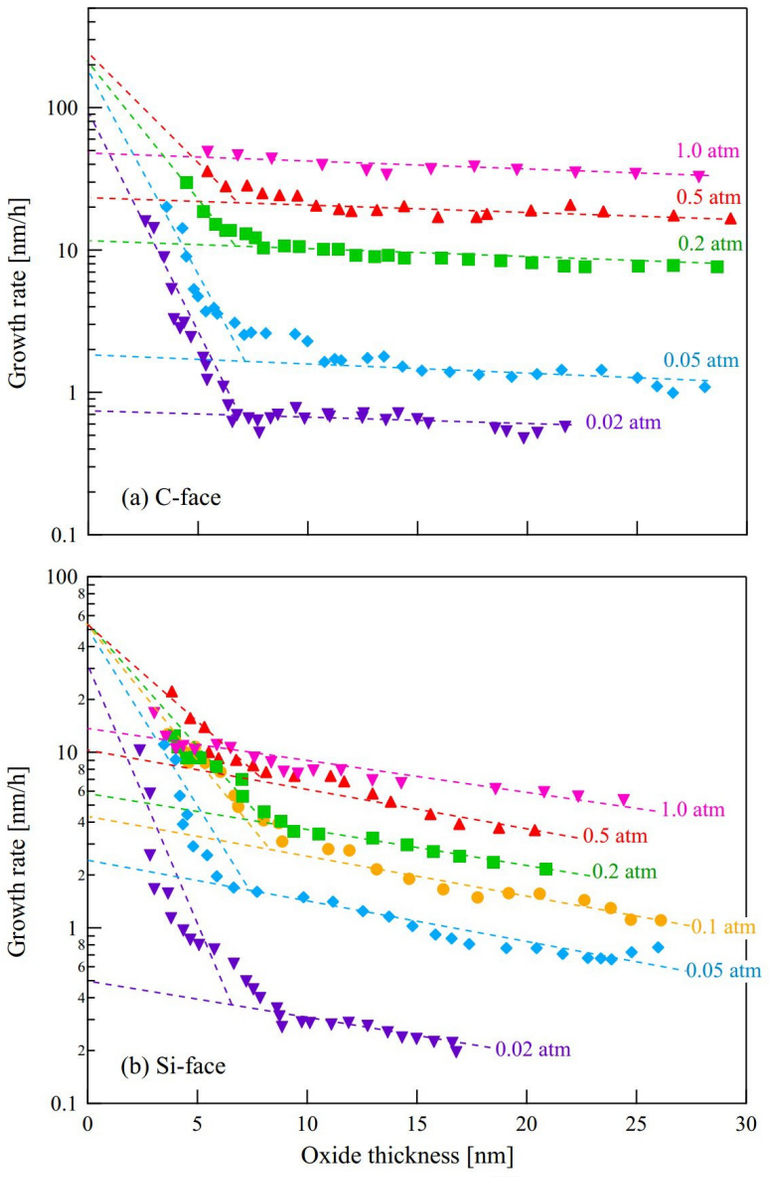

Figure 7. Oxide growth rates as a function of oxide thickness at various oxygen partial pressures on (000$\bar{1}$) C-face (a) and (0001) Si-face (b). The dashed lines are fitted to the experimental data using exponential functions.

Oxide thickness dependence of the oxide growth rates on 4H-SiC C-face (a) and Si-face (b) are shown in Fig. 7. As seen in the figure, we could obtain growth rate data in the extreme-thin oxide region down to a few nm more precisely by reducing the oxygen partial pressure less than 0.1 atm, compared with the case of measurements above 0.1 atm. For both faces, the oxide thickness dependence of growth rate less than 0.1 atm are basically similar to those of above 0.1 atm even if the partial pressure is lowered to 0.02 atm. Namely, just after the oxidation starts, the oxide growth rate rapidly decreases and at around 7 nm in thickness, the deceleration rate changes to gentle one (hereafter each oxidation stage is denoted as rapid and gentle deceleration stage, respectively). Because the growth rates at each of the deceleration stage well ride on a straight line in a semi-log plot (shown by dashed lines in

http://dx.doi.org/10.5772/50748

Fig. 7) in respective stage, the oxide thickness dependence of oxide growth rate can be approximated by a sum of the two exponential functions [11], as,

$$\frac{dX}{dt} = R_r \exp(-X / L_r) + R_g \exp(-X / L_g) \tag{11}$$

where, R_r and R_g ($R_r \gg R_g$) are pre-exponential constants, and L_r and L_g ($L_r < L_g$) are characteristic lengths for the deceleration of oxide growth rate in each oxidation stage. The first and the second terms represent the rapid and gentle deceleration stage, respectively. Equation (11) means that, in the thin oxide regime, the oxide growth occurs by two ways and these proceed not in series but in parallel because the growth rate is given by the sum of two terms and is determined mainly by the faster one in each stage. Obviously, the L_r and L_g values correspond to the gradients of the fitted line in the rapid and gentle deceleration stage, respectively. As shown in Fig. 7, the L_r value decreases with decreasing partial pressure, which corresponds to the more remarkable rapid deceleration. In contrast, the L_g value is almost constant regardless of the partial pressure. This suggests that the oxidation process is different between the rapid and gentle deceleration stage. It is noted that the thickness at which the deceleration rate changes from rapid one to gentle one (termed 'X_c') is almost constant around 7 nm regardless of oxygen partial pressure and surface polarity. In the case of Si oxidation, a rapid deceleration stage has also been observed just after oxidation starts, and the thickness corresponding to X_c is also almost independent of the oxygen partial pressure, though the growth rates at X_c depend on the oxygen partial pressure [13, 31]. Therefore, it can be stated that X_c is determined only by the thickness of the oxide layer for both the Si and SiC oxidation cases.

As mentioned above, the existence of a rapid deceleration stage in the oxide growth rate just after oxidation starts (X<10 nm) has been observed also for Si oxidation [13, 31]. However, in the investigations on Si oxidation mechanisms, the cause for the rapid deceleration has not been clarified yet, so far. For SiC oxidation, Yamamoto *et al.* have tried to reproduce the observed data using the Massoud's empirical equation [13]. Here, we will discuss the reasons why two deceleration stages exist in the thickness dependence of oxide growth rate, based on the Si and C emission model [19].

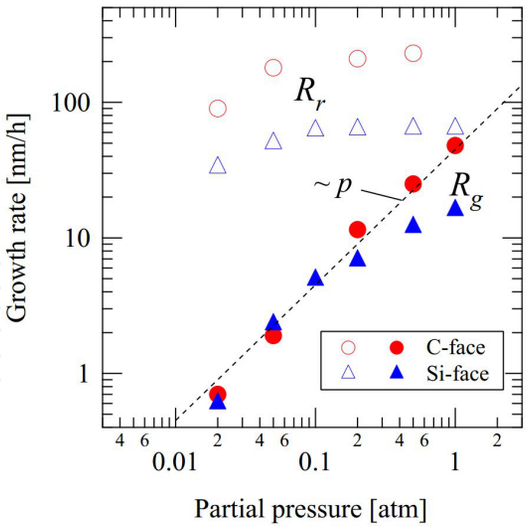

Figure 8. Oxygen partial pressure dependence of the initial growth rate, R_r (unfilled symbols), and the gentle deceleration growth rate, R_g (filled symbols), on C-face (circles) and Si-face (triangles).

We fitted the experimental data at each partial pressure with two straight lines, as shown by the dashed lines in Fig. 7, and derived the initial growth rate of the two deceleration stages, R_r and R_g, by extrapolating the straight line to X=0 in the rapid and the gentle deceleration stage, respectively. It is noticed that the meanings of R_r and R_g are the same as those in eq. (11). Figure 8 shows the oxygen partial pressure dependence of R_r and R_g, denoted by unfilled and filled symbols, respectively, on the C- (circles) and Si-faces (triangles). Since the oxide growth in thin thickness region was too fast to follow spectroscopic ellipsometry measurements in the case of 1 atm on C-face, we could not obtain the values of oxide growth rate in the rapid deceleration stage accurately, and thus the value of R_r for C face at 1 atm was not shown in this figure. The broken line in Fig. 8 shows the line proportional to oxygen partial pressure and fitted to the R_g data for C-face. For the both polar faces, the data points of R_g ride almost on the line, suggesting that R_g is proportional to partial pressure, though, for Si-face, R_g becomes slightly smaller as seen from the linear relation approaching 1 atm. It should be noted that the rates are almost equal to each other between C- and Si-faces at low pressure region, which is strangely different from the fact that the oxide growth rates for C-face are about eight times larger than those for Si-face at atmospheric oxygen pressure. If the oxide grows chiefly at the interface, the oxide growth rate dX/dt is rewritten by using eq. (6) as follows:

$$N_0 \frac{dX}{dt} \approx k C_O^I \tag{12}$$

The value of k is unlikely to depend on oxygen partial pressure because it corresponds to the rate that one SiC molecule is changed to one SiO_2 molecule, which should not depend on p. In the thin oxide regime discussed here, the interface oxygen concentration C_O^I can be ex-

http://dx.doi.org/10.5772/50748

pressed as $C_O^I \propto pC_O^0$ by Henry's low. Therefore, R, the growth rate when the oxide thickness X approaches 0, should be proportional to p, which is in good agreement with the experimental results in the gentle deceleration stage, *i.e.* R_g. Based on the Si emission model for Si oxidation (the Si and C emission model for SiC), the interface reaction rate k decreases with proceeding of oxidation due to the accumulation(s) of Si interstitials (Si and C interstitials). As the number of the accumulated atoms should increase with the proceeding of oxidation and thus is proportional to the quantity of oxidized molecules, *i.e.*, thickness of the oxide X, the variation in k may be approximately given as an exponential function of X in the form of $C\exp(-X/L)$, where C and L are the pre-exponential term and characteristic length, respectively, related to the accumulation(s) of Si (Si and C) interstitials at the interface. From these considerations as well as the fact that R_g is proportional to p, the gentle deceleration of oxide growth rate can be attributed to the accumulation(s) of Si (Si and C) interstitials near the interface, and given approximately as $dX/dt \propto R_g \exp(-X/L_g)$, which is coincident with the second term in eq. (11).

If the initial growth rate R_r in the rapid deceleration stage is also followed by eq. (12), it can be expressed that $R_r = k_0' C_O^I / N_0$, where k_0' is the interfacial reaction rate when oxidation starts. As the value of k_0' is also unlikely to depend on oxygen partial pressure, R_r should be also proportional to oxygen pressure. While, as seen in Fig. 8, R_r is not proportional to p, though it decreases with decreasing p in the low p region. Also in the case of Si oxidation, the experimental data show almost no dependency of R_r with respect to p [13]. Here, we consider the reason why R_r is not proportional to but almost independent of oxygen partial pressure both for Si and SiC oxidation.

It has been considered that oxide growth occurs only or mainly at the Si-oxide (SiC-oxide) interface, so far. However, according to the interfacial Si emission model [14, 17] for Si oxidation and the Si and C emission model [19] for SiC oxidation, Si atoms (Si and C atoms) emit into the oxide layer, and some of which meet with oxidant inside the oxide to form SiO_2. When the thickness of the oxide is very thin, a part of the emitted Si atoms can go through the oxide layer and reach the oxide surface, and then are instantly oxidized, resulting in the formation of a SiO_2 layer on the oxide surface. Therefore, there are two oxide growth processes other than the interfacial oxide growth, *i.e.*, the oxide formation due to the oxidations of Si interstitials on the oxide surface and inside the oxide, and the total growth rate is given by the sum of these three oxidation processes, as revealed in eq. (6). In the case of oxidation inside the oxide, the possibility that an emitted Si interstitial encounter oxygen inside the oxide should be proportional to the oxygen concentration in the oxide. Therefore, this oxidation process should be proportional to p like R_g, and thus, can be excluded as a candidate of the origin of R_r. In contrast, in the case of oxidation on the oxide surface, the amount of oxygen is thought to be enough to oxidize all the Si atoms emitted and appearing on the surface, because the number of oxygen molecules impinging onto the surface from the gaseous atmosphere is several orders larger than that of emitted Si atoms transmitted through oxide even if the oxygen pressure is as low as 0.02 atm[1]. Therefore, the oxide

growth rate for the oxidation on the oxide surface should be independent of the oxygen partial pressure, which is in good agreement with the behavior of R_r. Besides, the possibility that Si interstitials go through the oxide and reach the oxide surface is considered to decrease rapidly with increasing oxide thickness, and can be given as a form of $\exp(-X/L_r)$, where L_r ($<L_g$) is the escape depth of Si atoms from the oxide layer. From these considerations, the rapid deceleration stage of oxide growth rate observed just after oxidation starts is thought to be due to oxidation of Si interstitials on the oxide surface. The value of X_c obtained from the experiments, around 7 nm, indicates that the escape depth of Si from the oxide is estimated to be several nm at 1100°C.

As has been mentioned above, in the rapid deceleration stage, the growth rate is determined with the oxidation rate of the emitted Si interstitials on the oxide surface (termed 'surface oxide growth'), while in the gentle deceleration stage, it is determined by the oxidation rate at the SiC-oxide interface and that of the emitted Si interstitials inside the SiO_2 layer (termed 'interfacial oxide growth' and 'internal oxide growth', respectively). The surface oxide growth rate depends little on partial pressure and, in contrast, the interfacial and internal oxide growth rates are proportional to partial pressure. It is therefore predicted from these pressure dependence that the rapid deceleration becomes more remarkable (*i.e.* the smaller L_r) at lower partial pressures, which is confirmed in Fig. 7. In addition, the reason why the growth rates in the rapid deceleration stage at low pressures are not so much different between C- and Si-faces is that the surface oxide growth is dominant to the oxide growth in this stage, so that the oxidation on the oxide surface may proceed independently of the surface polarity.

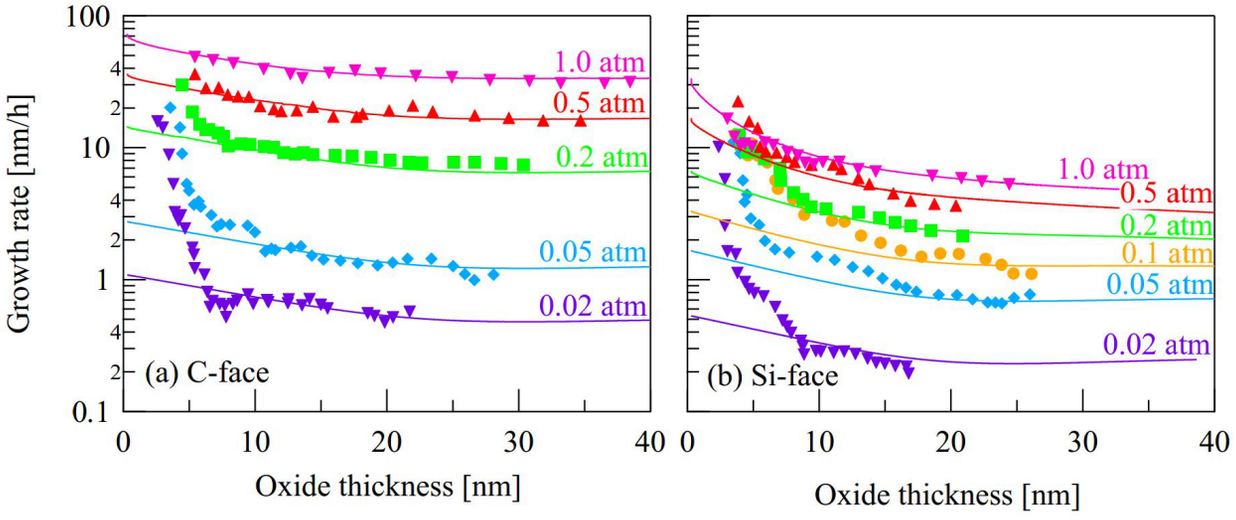

Figure 9. Oxide growth rates as a function of oxide thickness at various oxygen partial pressures on $(000\bar{1})$ C-face (a) and (0001) Si-face (b). The solid lines denote growth rates given by the Si and C emission model [19].

1 The oxygen flux impinging from a gaseous atmosphere of pressure p to the solid surface is $3\times10^{22}p[m^{-2}s^{-1}]$. Since the areal density of Si atoms on SiO_2 is about $8\times10^{18}[m^{-2}]$, the flux in the case that p=0.02 atm corresponds to 75 [monolayer/s], which is the oxygen flux necessary for the oxide growth rate of 105 nm/h.

Figure 9 compares the observed oxide growth rates at various oxygen partial pressures on SiC (000$\bar{1}$) C-face (a) and (0001) Si-face (b) with the growth rates given by the Si and C emission model (solid lines). It is noted that all the parameters used in the calculations other than the solubility limit of oxygen in SiO_2 [2] are the same regardless of partial pressures. The figures indicate that the calculated curves successfully reproduce the observed growth rates though restricted in the gentle deceleration region and that the calculated curves show the rapid reduction more remarkable as the higher partial pressure, which is opposite tendency to that of the observed data. Also in the case of Si oxidation, the interfacial Si emission model [14, 17] cannot reproduce the growth rate in the thin oxide region at sub-atmospheric pressure, as pointed out by Farjas and Roura [31]. We consider that the accurate description for the surface oxide growth may dissolve the disagreement between the calculated and observed oxide growth rates in the cases of low partial pressures. To verify this idea, we separately calculated the oxide growth rate on the surface, inside the SiO_2 layer, and at the SiC-SiO_2 interface (denoted asF_{sur}, F_{ox}, andF_{int}, respectively) using the Si and C emission model.

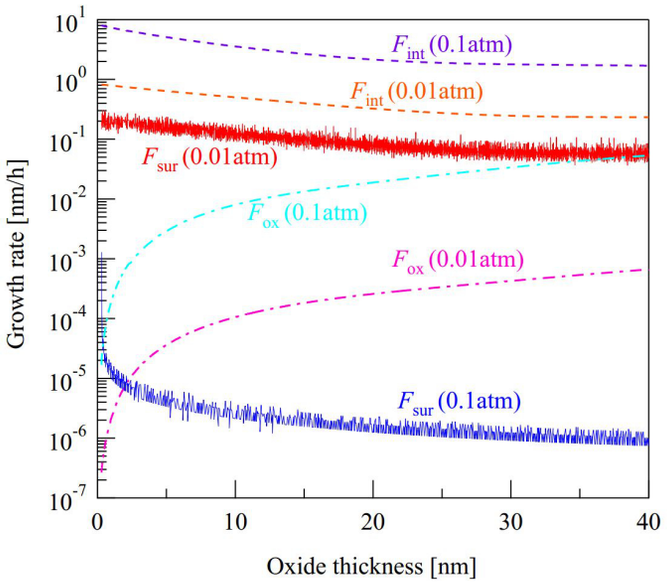

Figure 10. Simulated oxide growth rates on the surface, inside the SiO_2 layer, and at the SiC-SiO_2 interface (F_{sur}, F_{ox}, andF_{int}, respectively) at 0.1 and 0.01 atm on Si-face.

Figure 10 shows the calculation results ofF_{sur}, F_{ox}, and F_{int} at 0.1 and 0.01 atm on Si-face. The figure indicates that the F_{sur} curve for 0.01 atm is much higher than that for 0.1 atm by a factor of about 5 orders, though the F_{sur} is still lower thanF_{int}. This result confirms that the low pressure oxidation enhances the oxide growth on the surface, as discussed above, which is probably due to the reduction in the oxygen concentration at the interface and inside the oxide. Conversely, the F_{ox} and F_{int} curves for 0.01 atm are lower than those for 0.1 atm by factors of 2 orders and 1 order, respectively. Since the F_{int} is higher than F_{ox} in general, it is

2 The corresponding solubility limit of oxygen is derived by multiplying partial pressure by that for 1 atm, *i.e.*, $C_O^0 = p \times C_O^0$ (1 atm).

found that the growth rate in the gentle deceleration stage to be proportional to pressure is due to the proportional increase inF_{int}. Moreover, a careful look confirms the deceleration of F_{int} in the very-thin oxide region (*ca.*< 5 nm) to be enhanced as elevating the pressure, which has been seen in the calculated curves in Fig. 9. Therefore, it is necessary for the Si and C emission model, as well as for the interfacial Si emission model that an appropriate description for the oxide growth on the surface is introduced to the model so as to enhance the surface growth rate in the initial oxidation region up to over the interfacial growth rate.

3.4. Discussion on Si and C emission phenomenon and its relation to the interface layer

So far, we specify the oxidation mechanism of SiC from the viewpoint of the Si and C emission phenomenon. In this section, we will discuss the structure and the formation mechanism of the interface layer between SiC-SiO_2, which has been considered as the crucial issue for the practical use of SiC-MOSFET, in the light of interfacial Si and C emission.

In previous work, we have found that [32, 33] the photon energy dependence of the optical constants n and k of the interface layer derived from the complex dielectric constants between 2 and 6 eV, covering the direct interband transition energy E_0 of 4H-SiC of 5.65 eV, is similar to that of bulk 4H-SiC, though the absolute values of n are about 1 larger than those of SiC [34]. We also found from the real time observation of SiC oxidation process using an *in-situ* spectroscopic ellipsometry that [30] the interface layer thickness increases with increasing oxide thickness and saturates around 1.5 nm at the oxide thickness of around 7 nm, and the refractive indices of the layer are also saturated at around 7 nm in oxide thickness to the similar values obtained from *ex-situ* measurements. The similarity in the energy dispersion of the optical constants of the interface layers suggests that the interface layer is not a transition layer between SiC and SiO_2, such as SiO_x or SiC_xO_y. Rather, it is a layer having a modified structure and/or composition compared to SiC, such as a stressed or interstitials-incorporated SiC layer, locating not on the SiO_2 side but the SiC side of the SiC-oxide interface.

According to the results from the real time observation [30], the thickness at which the interface layer thickness and the refractive index become constant (*i.e.*, 7 nm) is determined not from the surface polarity or oxygen partial pressure but from the oxide thickness. The Si and C emission model describes this behavior by considering that Si and C atoms are emitted into both directions of the SiC-oxide interface accompanying oxidation at the interface, *i.e.*, into not only the oxide layer but also the SiC layer (see Fig. 2), and accumulation of interstitial Si and/or C atoms emitted into the SiC substrate may form a layer having similar optical properties as SiC but larger refractive indices compared to SiC. Since accumulation of interstitials is linked to the growth of the oxide, it is considered that growth of the interface layer is saturated at some intrinsic oxide thickness even if the oxygen pressure is changed. Takaku *et al.* have found from the real time observation that the use of relatively low oxidation temperature or oxygen pressure leads to no formation of the interface layer [35], which can be explained by considering that the accumulations of Si and/or C interstitials are prevented by lowering the temperature or pressure.

Hashimoto *et al.* have found that there is a strong correspondence between the refractive index of the interface layer and interface state density obtained from the MOS capacitors fabricated on the same sample for ellipsometry measurements [32]. Hence, we believed that the accumulations of Si and C interstitials near/at the interface are closely related to the formation of interface states. According to the report from Afanasev *et al.* [36], a graphite-like carbon layer forms near/at the interface, which causes interface states over the whole range of forbidden energy band and, in addition, an intrinsic SiO_2 defect (NIT: near interface trap), presumably originating from oxygen deficiency, exists regardless of Si or SiC-polytypes and gives rise to the interface states in the vicinity of the 4H-SiC conduction band edge, which cause a channel degradation in MOSFETs. Since the oxygen deficiency can be regarded as a Si interstitial in SiO_2, Si (Si and C) emission into SiO_2 layer may be the origin for this SiO_2 defect. According to the *ab-initio* studies performed by Knaup *et al.* [37], the origin of NITs is Si interstitials or C dimers originating from C interstitials inside SiO_2. They also reported that C dimers in the SiC-side give rise to interface states at the energy range between mid gap and valence band edge. On the other hand, according to the *ab-initio* studies from Devynck *et al.* [38], C-C pair in SiC originating from C interstitials and a Si-C-O structure give rise to a broad peak of interface state density, and a Si_2-C-O structure give rise to a sharp peak near the conduction band edge, which is compatible with NIT. Cochrane *et al.* have performed an Electrically detected magnetic resonance (EDMR) techniques and found Si vacancies (or C dangling bonds) in the SiC-side near the interface [40], which is presumably attributed to the Si emission during oxidation. Very recently, Shen and Pantelides have reported that they identified the origin of interface states that degrade the SiC MOS channel mobility as 'C di-interstitials', which are formed by a combination of the two C interstitials injected into the SiC [41]. Accordingly, we tried to simulate the formation of the interface layer based on the diffusion theory and, as a result, the calculations reproduced the interface layer with the thickness of around 1 nm [39], which agrees with the values often reported [18, 34, 39]. Anyway, we would like to emphasize here that further understanding of the interfacial Si and C emission phenomenon during oxidation of SiC might be the key to realize the intrinsic performances of SiC MOSFETs.

Finally, we would like to introduce a recent innovation using oxidation about elimination of point defects. Hiyoshi and Kimoto invented an epoch-making idea, in which as-grown deep-level states such as a $Z_{1/2}$ center can be eliminated by oxidation of SiC substrates [43]. Taking into account the report from Storasta *et al.* [44] in which the origin of $Z_{1/2}$ is perhaps C vacancy, Hiyoshi and Kimoto considered the mechanism of deep-level state elimination by oxidation as follows: The excess silicon and carbon interstitials may be generated at the oxidizing interface, and a part of the emitted silicon and carbon interstitials may diffuse into the epilayer, and consequently, recombination of the interstitials with vacancies present in the epilayers may take place [45]. Therefore, the Si and C emission surely takes place during oxidation and the survey of Si and C interstitial movement is very important to utilize thermal oxidation as a device fabrication process, *e.g.* Ref. [46], even in the developments in bipolar devices of over 10 kV class. Very recently, we found that stacking-faults are formed or extended by thermal oxidation, which is perhaps induced by the interfacial strain due to thermal oxidation [47].

4. Conclusion

We review the oxidation mechanism of SiC and the formation of the interface layer between SiC and SiO_2. Though most of articles have reported that the Deal-Grove model also describes the SiC oxidation process, we pointed out the discrepancy in the application of Deal-Grove model, in which the oxide growth rate in the thin oxide region cannot be reproduced with this model. Aimed at the elucidation of SiC oxidation process in this thin oxide region, we proposed a kinetic model that accounts for SiC oxidation, termed the 'Si and C emission model', and showed that the model well reproduces the oxide growth rate over the entire thickness range including the thin oxide region for both the C and Si faces. The results indicated that the oxidation and emission of C and the emission of Si all need to be taken into account to describe the oxide growth process in SiC. A comparison of the parameters obtained for the C and Si faces from the curve fits revealed that the differences in initial interfacial reaction rate and Si emission ratio are contributing to the large difference in oxide growth rate between these polar faces.

We tried to apply the Si and C emission model to the oxide growth rate data at various oxidation temperatures and found that the model reproduces the oxide growth rate curves for all of the temperatures measured for both of the Si- and C-faces. Comparing with the parameters deduced from the curve fits, we discussed the differences in oxidation process between Si- and C-face. We also showed the parameters obtained in this study, some of which such as a diffusivity and solubility limit of C in SiO_2 were firstly reported.

We have studied the oxygen partial pressure dependence of the SiC oxidation process on the Si- and C-faces. The oxide thickness dependence of the growth rate at sub-atmospheric oxygen partial pressures down to 0.02 atm show that, just after oxidation starts, the oxide growth rate rapidly decreases and the deceleration-rate changes to a gentle mode at around 7 nm in oxide thickness, which are probably the oxide surface growth mode and oxide internal/interfacial growth mode, respectively. We tried to reproduce the pressure dependence of oxide growth rates, however, it cannot be achieved, which is perhaps due to the inaccurate description for the oxide growth on the oxide surface.

Finally, we discussed the structure and formation mechanism of the SiC–oxide interface layer in terms of the Si and C emission phenomenon. We also introduced a recently invented technology on defect using oxidation, *i.e.* point defect elimination by oxidation, and suggested that understanding of oxidation mechanism is also very important in the developments of SiC bipolar devices.

Acknowledgements

The authors would like to thank Professor Uematsu of Keio University and Dr. Kageshima of NTT for their helpful advice and technical support for the simulation. This work was partially supported by a Grant-in-Aid for Scientific Research (24560365) from the Japan Society for the Promotion of Science.

Author details

Yasuto Hijikata[1*], Shuhei Yagi[1], Hiroyuki Yaguchi[1] and Sadafumi Yoshida[2]

*Address all correspondence to: yasuto@opt.ees.saitama-u.ac.jp

1 Division of Mathematics Electronics and Informatics, Graduate School of Science and Engineering, Saitama University, Japan

2 Advanced Power Electronics Research Center, National Institute of Advanced Industrial Science and Technology, Japan

References

[1] Yoshida, S. (2000). *Electric Refractory Materials*, ed. Y. Kumashiro (Dekker, New York), 437.

[2] Matsunami, H. (2004). Technological Breakthroughs in Growth Control of Silicon Carbide for High Power Electronic Devices. *Jpn. J. Appl. Phys.*, 43(1), 6835-6847.

[3] Afanas'ev, V. V., & Stesmans, A. (1997). H-complexed oxygen vacancy in SiO_2: Energy level of a negatively charged state. *Appl. Phys. Lett.*, 71, 3844-3846.

[4] Hijikata, Y., Yaguchi, H., & Yoshida, S. (2011). *Properties and Applications of Silicon Carbide*, ed. R. Gerhardt (INTECH open access publisher, 2011) chapter 4.

[5] Kakubari, K., Kuboki, R., Hijikata, Y., Yaguchi, H., & Yoshida, S. (2006). Real Time Observation of SiC Oxidation using In-Situ Ellipsometer. *Mater. Sci. Forum*, 527-529, 1031-1034.

[6] Deal, B. E., & Grove, A. S. (1965). General Relation Ship for the Thermal Oxidation of Silicon. *J. Appl. Phys.*, 36, 3770-3778.

[7] Song, Y., Dhar, S., Feldman, L. C., Chung, G., & Williams, J. R. (2004). Modified Deal Grove model for the thermal oxidation of silicon carbide. *J. Appl. Phys.*, 95, 4953-4957.

[8] Yamamoto, T., Hijikata, Y., Yaguchi, H., & Yoshida, S. (2007). Growth Rate Enhancement of ($000\bar{1}$)-Face Silicon-carbide Oxidation in Thin Oxide Regime. *Jpn. J. Appl. Phys*, 46, L770-L772.

[9] Yamamoto, T., Hijikata, Y., Yaguchi, H., & Yoshida, S. (2008). Oxide Growth Rate Enhancement of Silicon Carbide (0001) Si-Faces in Thin Oxide Regime. *Jpn. J. Appl. Phys.*, 47, 7803-7806.

[10] Yamamoto, T., Hijikata, Y., Yaguchi, H., & Yoshida, S. (2008). Oxygen-Partial-Pressure Dependence of SiC Oxidation Rate Studied by In-situ Spectroscopic Ellipsometry. *Mater. Sci. Forum*, 600-603, 667-670.

[11] Kouda, K., Hijikata, Y., Yaguchi, H., & Yoshida, S. (2010). In-situ Spectroscopic Ellipsometry Study of SiC Oxidation at Low Oxygen-Partial-Pressures. *Mater. Sci. Forum*, 645-648, 813-816.

[12] Grove, A. S. (1967). *Physics and Technology of Semiconductor Devices*, John Wiley & Sons, New York, 31.

[13] Massoud, H. Z., Plummer, J. D., & Irene, E. A. (1985). Thermal Oxidation of Silicon in Dry Oxygen: Growth-Rate Enhancement in the Thin Regime: I. Experimental Results. *J. Electrochem. Soc.*, 132, 2685-2693, Thermal Oxidation of Silicon in Dry Oxygen: Growth-Rate Enhancement in the Thin Regime: II. Physical Mechanism, ibid 132, 2693-2700.

[14] Kageshima, H., Shiraishi, K., & Uematsu, M. (1999). Universal Theory of Si Oxidation Rate and Importance of Interfacial Si Emission. *Jpn. J. Appl. Phys.*, 38(2), L971-L974.

[15] Ogawa, S., & Takakuwa, Y. (2006). Rate-Limiting Reactions of Growth and Decomposition Kinetics of Very Thin Oxides on Si(001) Surfaces Studied by Reflection High-Energy Electron Diffraction Combined with Auger Electron Spectroscopy. *Jpn. J. Appl. Phys.*, 45, 7063-7079.

[16] Watanabe, T., Tatsumura, K., & Ohdomari, I. (2006). New Linear-Parabolic Rate Equation for Thermal Oxidation of Silicon. *Phys. Rev. Lett.*, 96, 196102-1-196102-4.

[17] Uematsu, M., Kageshima, H., & Shiraishi, K. (2001). Simulation of wet oxidation of silicon based on the interfacial silicon emission model and comparison with dry oxidation. *J. Appl. Phys.*, 89, 1948-1953.

[18] Hijikata, Y., Yaguchi, H., Yoshida, S., Takata, Y., Kobayashi, K., Nohira, H., & Hattori, T. (2006). Characterization of Oxide Films on 4H-SiC Epitaxial ($000\bar{1}$) Faces by High-Energy-Resolution Photoemission Spectroscopy: Comparison between Wet and Dry Oxidation. *J. Appl. Phys.*, 100, 053710-1-053710-6.

[19] Hijikata, Y., Yaguchi, H., & Yoshida, S. (2009). A Kinetic Model of Silicon Carbide Oxidation Based on the Interfacial Silicon and Carbon Emission Phenomenon. *Appl. Phys. Express*, 2, 021203-1-021203-3.

[20] Uematsu, M., Kageshima, H., & Shiraishi, K. (2000). Simulation of High-Pressure Oxidation of Silicon Based on the Interfacial Silicon Emission Model. *Jpn. J. Appl. Phys.*, 39, L952-L954.

[21] Sze, S. M. (2002). *Semiconductor Devices Physics and Technology*, John Wiley & Sons, Inc., New Jersey, 2nd ed., Chap. 13, 457.

[22] Jügling, W., Pichler, P., Selberherr, S., Guerrero, E., & Pötzel, H. W. (1985). Simulation of Critical IC Fabrication Processes Using Advanced Physical and Numerical Methods. *IEEE Trans. Electron. Devices*, 32, 156-167.

[23] Ray, E. A., Rozen, J., Dhar, S., Feldman, L. C., & Williams, J. R. (2008). Pressure dependence of SiO_2 growth kinetics and electrical properties on SiC. *J. Appl. Phys.*, 103, 023522-1-023522-7.

[24] Hijikata, Y., Yamamoto, T., Yaguchi, H., & Yoshida, S. (2009). Model Calculation of SiC Oxidation Rates in the Thin Oxide Regime. *Mater. Sci. Forum*, 600-603, 663-666.

[25] Hijikata, Y., Yaguchi, H., & Yoshida, S. (2010). Model calculations of SiC oxide growth rate at various oxidation temperatures based on the silicon and carbon emission model. *Mater. Sci. Forum*, 645-648, 809-812.

[26] Szilágyi, E., Petrik, P., Lohner, T., Koós, A. A., Fried, M., & Battistig, G. (2008). Oxidation of SiC investigated by ellipsometry and Rutherford backsccatering spectrometry. *J. Appl. Phys.*, 104, 014903-1-014903-7.

[27] Hijikata, Y., Yaguchi, H., & Yoshida, S. (2009). Model Calculation of SiC Oxide Growth Rate based on the Silicon and Carbon Emission Model. *Mater. Sci. Forum*, 615-617, 489-492.

[28] Zheng, Z., Tressler, R. E., & Spear, K. E. (1990). Oxidation of Single-Crystal Silicon Carbide. *J. Electrochem. Soc.*, 137, 854-858.

[29] Krafcsik, O. H., Vida, G., Pócsik, I., Josepovits, K. V., & Deák, P. (2001). Carbon Diffusion through SiO_2 from a Hydrogenated Amorphous Carbon Layer and Accumulation at the SiO_2 / Si Interface. *Jpn. J. Appl. Phys.*, 40, 2197-2200.

[30] Kouda, K., Hijikata, Y., Yagi, S., Yaguchi, H., & Yoshida, S. Oxygen partial pressure dependence of the SiC oxidation process studied by in-situ spectroscopic ellipsometry. *J. Appl. Phys*, accepted for publication.

[31] Farjas, J., & Roura, P. (2007). Oxidation of silicon: Further tests for the interfacial silicon emission model. *J. Appl. Phys.*, 102, 054902-1-054902-8.

[32] Hashimoto, H., Hijikata, Y., Yaguchi, H., & Yoshida, S. (2009). Optical and Electrical Characterizations of 4H-SiC-Oxide interfaces by Spectroscopic Ellipsometry and Capacitance-Voltage measurements. *Appl. Surf. Sci.*, 255, 8648-8653.

[33] Seki, H., Hijikata, Y., Yaguchi, H., & Yoshida, S. (2009). Characterization of 4H-SiC-SiO_2 Interfaces by a Deep Ultraviolet Spectroscopic Ellipsometer. *Mater. Sci. Forum*, 615-617, 505-508.

[34] Iida, T., Tomioka, Y., Midorikawa, M., Tsukada, H., Orihara, M., Hijikata, Y., Yaguchi, H., Yoshikawa, M., Itoh, H., Ishida, Y., & Yoshida, S. (2002). Measurement of the depth profile of the refractive indices in the oxide films on SiC by spectroscopic ellipsometry. *Jpn. J. Appl. Phys.*, 41(1), 800-804.

[35] Takaku, T., Hijikata, Y., Yaguchi, H., & Yoshida, S. (2009). Observation of SiC Oxidation in Ultra-Thin Oxide Regime by In-situ Spectroscopic Ellipsometry. *Mater. Sci. Forum*, 615-617, 509-512.

[36] Afanasev, V. V., Bassler, M., Pensl, G., & Shulz, M. (1997). Intrinsic SiC/SiO_2 Interface States. *Phys. stat. sol. (a)*, 162, 321-337.

[37] Knaup, J. M., Deák, P., Frauenheim, Th., Gari, A., Hajnal, Z., & Choyke, W. J. (2005). Theoretical study of the mechanism of dry oxidation of 4H-SiC. *Phys. Rev. B*, 71, pp. 235321-1-9, Defects in SiO_2 as the possible origin of near interface traps in the $SiC-SiO_2$ system: A systematic theoretical study, ibid, 72, 115323-1-9.

[38] Devynck, F., Alkauskas, A., Broqvist, P., & Pasquarello, A. (2011). Defect levels of carbon-related defects at the SiC/SiO_2 interface from hybrid functionals. *Phys. Rev. B*, 83, pp. 195319-1-11, Charge transition levels of carbon-, oxygen-, and hydrogen-related defects at the SiC/SiO_2 interface through hybrid functionals, ibid, 84, 235320-1-18.

[39] Cochrane, C. J., Lenahan, P. M., & Lelis, A. J. (2011). An electrically detected magnetic resonance study of performance limiting defects in SiC metal oxide semiconductor field effect transistors. *J. Appl. Phys.*, 109, 014506-1-014506-12.

[40] Shen, X., & Pantelides, S. T. (2011). Identification of a major cause of endemically poor mobilities SiC/SiO_2 structures. *Appl. Phys. Lett.*, 98, 0535071-1-0535071-3.

[41] Hijikata, Y., Yaguchi, H., & Yoshida, S. (2011). Theoretical studies for Si and C emission into SiC layer during oxidation. *Mater. Sci. Forum*, 679-680, 429-432.

[42] Hijikata, Y., Yaguchi, H., Yoshikawa, M., & Yoshida, S. (2001). Composition analysis of SiO_2/SiC interfaces by electron spectroscopic measurements using slope-shaped oxide films. *Appl. Surf. Sci.*, 184, 161-166.

[43] Hiyoshi, T., & Kimoto, T. (2009). Reduction of Deep Levels and Improvement of Carrier Lifetime in n-Type 4H-SiC by Thermal Oxidation. *Appl. Phys. Express*, 2, pp. 041101-1-3.

[44] Storasta, L., Tsuchida, H., & Miyazawa, T. (2008). Enhanced annealing of the $Z_{1/2}$ defect in 4H-SiC epilayers. *J. Appl. Phys.*, 103, 013705-1-013705-7.

[45] Hiyoshi, T., & Kimoto, T. (2009). Elimination of the Major Deep Levels in n- and p-Type 4H-SiC by Two-Step Thermal Treatment. *Appl. Phys. Express*, 2, 091101-1-091101-3.

[46] Kawahara, K., Suda, J., & Kimoto, T. (2012). Analytical model for reduction of deep levels in SiC by thermal oxidation. *J. Appl. Phys.*, 111, 053710-1-053710-9.

[47] Yamagata, H., Yagi, S., Hijikata, Y., & Yaguchi, H. (2012). Micro-Photoluminescence study on the influence of oxidation on stacking faults in 4H-SiC epilayers. *Appl. Phys. Express.*, 5, 051302-1-051302-3.